

Lawrence Berkeley National Laboratory

LBL Publications

Title

Activation of carbon dioxide by a terminal uranium–nitrogen bond in the gas-phase: a demonstration of the principle of microscopic reversibility

Permalink

<https://escholarship.org/uc/item/85f7q5hm>

Journal

Physical Chemistry Chemical Physics, 18(10)

ISSN

1463-9076

Authors

Dau, Phuong D
Armentrout, PB
Michelini, Maria C
[et al.](#)

Publication Date

2016-03-14

DOI

10.1039/c6cp00494f

Copyright Information

This work is made available under the terms of a Creative Commons Attribution-NonCommercial-NoDerivatives License, available at <https://creativecommons.org/licenses/by-nc-nd/4.0/>

Peer reviewed

**Activation of Carbon Dioxide by a Terminal Uranium-Nitrogen Bond in the Gas-Phase:
A Demonstration of the Principle of Microscopic Reversibility**

Phuong D. Dau,¹ P. B. Armentrout,² Maria C. Michelini,³ John K. Gibson^{1,*}

¹ Chemical Sciences Division, Lawrence Berkeley National Laboratory, Berkeley, California, 94720, United States

² Department of Chemistry, University of Utah, Salt Lake City, Utah 84112-0850, United States

³ Dipartimento di Chimica, Università della Calabria, 87030 Arcavacata di Rende, Italy

*Email: jkgibson@lbl.gov

Abstract

Activation of CO₂ is demonstrated by its spontaneous dissociative reaction with the gas-phase anion complex NUOCl₂⁻, which can be considered as NUO⁺ coordinated by two chloride anion ligands. This reaction was previously predicted by density functional theory to occur exothermically, without barriers above the reactant energy. The present results demonstrate the validity of the prediction of microscopic reversibility, and provide a rare case of spontaneous dissociative addition of CO₂ to a gas-phase complex. The activation of CO₂ by NUOCl₂⁻ proceeds by conversion of a U≡N bond to a U=O bond and creation of an isocyanate ligand to yield the complex UO₂(NCO)Cl₂⁻, in which uranyl, UO₂²⁺, is coordinated by one isocyanate and two chloride anion ligands. This activation of CO₂ by a uranium(VI) nitride complex is distinctive from previous reports of oxidative insertion of CO₂ into lower oxidation state U(III) or U(IV) solid complexes, during which both C-O bonds remain intact. This unusual observation of spontaneous addition and activation of CO₂ by NUOCl₂⁻ is a result of the high oxophilicity of uranium. If the computed free energy of the reaction pathway, rather than the energy, is considered, there are barriers above the reactant asymptotes such that the observed reaction should not proceed under thermal conditions. This result provides a demonstration that energy rather than free energy determines reactivity under low-pressure bimolecular conditions.

Introduction

Although endothermic activation of carbon dioxide occurs on a massive scale in photosynthesis, it presents a particular challenge in synthetic chemistry because of the very strong C-O bonds: $\text{CO}_2 + 1609 \text{ kJ}\cdot\text{mol}^{-1} \rightarrow \text{C} + 2\text{O}$.¹ A classic example of efficient activation of CO_2 is the conversion of calcium oxide to calcium carbonate: $\text{CaO}(\text{s}) + \text{CO}_2(\text{g}) \rightarrow \text{CaCO}_3(\text{s})$.² More recent studies have focused on controlled activation by metal complexes, with goals of reducing the amount of atmospheric CO_2 , and/or enhancing its utility as an abundant and cheap C_1 precursor for large-scale chemical synthesis.³ There are several examples of CO_2 insertion into metal complexes, including lanthanide pentamethylcyclopentadienyls,⁴ a zinc hydride,⁵ a Ru ONP-pincer,⁶ and a lithium polynitride.⁷ There has been considerable effort towards disrupting the C-O bond with resulting C-C or C-N bond formation.⁸⁻¹⁰ An elegant example is the conversion of CO_2 to CO catalyzed by an anionic niobium nitride complex.¹¹ Recently, Group 6 imido complexes have been demonstrated as intermediates in the catalytic conversion of CO_2 to isocyanates, $\text{R}_3\text{EN}=\text{C}=\text{O}$ (E = C, Si, Ge),¹² a process that is directly relevant to the present work.

Uranium complexes have received substantial attention for providing new catalytic pathways, including activation of small molecules, and CO_2 in particular.¹³⁻¹⁶ A few especially important and representative examples are mentioned here. More than 40 years ago, Bagnall and Yanir demonstrated that CO_2 inserts into the U-N bonds of uranium(IV)dialkylamides to yield carbamates.¹⁷ In recent years there has been a resurgence in this field. In 2004, Meyer and co-workers discovered that the reaction of a U(III) tris(aryloxy) complex with CO_2 produces a terminally bound $\eta^1\text{-CO}_2$ complex.¹⁸ Subsequently, Bart et al. reported a detailed study of the insertion of CO_2 into U(IV)-N amide bond to produce carbamates, and U(V)-N amide bond to produce uranium(V) terminal oxo species and isocyanates.¹⁹ Arnold and co-workers have reported on the activation of CO_2 by uranium tris(aryloxides),²⁰ as well as by a uranium N-heterocyclic carbene and uranium tris amides $\text{U}\{\text{N}(\text{SiMe}_3)_2\}_3$ to yield an isocyanate.²¹ Bart and co-workers reported the insertion of CO_2 into U-C, U-N and U-S bonds to form carboxylates or carbamates.²² Kahan et al. reported reductive insertion of CO_2 into sandwich U(III) complexes.²³ As a final example, Evans and co-workers demonstrated insertion of CO_2 into U(IV) organometallic complexes to produce carboxylates.²⁴

Activation of CO_2 in the gas phase has been studied by several groups. Abstraction of an O atom from CO_2 by bare and oxo-ligated metal ions has been reported.^{25, 26} Koyanagi and Bohme demonstrated that several transition metal ions, M^+ , exothermically abstract an oxygen atom to produce MO^+ and CO.²⁷ Sievers and Armentrout studied reactions of V^+ , Y^+ , Nb^+ , YO^+ and NbO^+ with CO_2 by guided ion beam mass spectrometry to reveal fundamental aspects of CO_2 activation.²⁸⁻³⁰ Armentrout and Beauchamp, and later Marçalo and co-workers, demonstrated that U^+ exothermically reacts with CO_2 to yield UO^+ and CO.^{31, 32} Metal cluster cations (Fe, Cr) have been shown to activate CO_2 at thermal energies to form metal oxide clusters and release CO.^{33, 34} Schwarz and co-workers, as well as other groups, have studied several elementary reactions in the gas phase to model and understand the activation of CO_2 .³⁵⁻³⁹

A particularly notable result is the coupling of CH₄ and CO₂ mediated by Ta⁺: Ta⁺ reacts with CH₄ to yield TaCH₂⁺, which then sequentially reacts with two CO₂ molecules to yield TaO₂⁺ and C₂H₂O; the latter is inferred to be the ketene, H₂C=C=O, in which carbon-carbon coupling has been achieved.³⁶ To the best of our knowledge there is as of yet no demonstration of direct and spontaneous insertion and retention of CO₂ in a gas-phase complex concomitant with activation of a C-O bond.

In the work reported here, the ability of uranium to activate CO₂ in the gas phase is further explored, with a goal beyond oxygen atom abstraction. In view of the very strong uranium-oxygen bonds,⁴⁰ it may be feasible to enable CO₂ activation by formation of a U-O bond, along with another stable fragment. It has recently been demonstrated that the U=O bond of uranyl can be converted to a U≡N bond in the gas phase,^{41, 42} to yield the N≡U=O⁺ moiety, an elusive transformation in condensed phase.⁴³ The utility of such gas-phase endothermic decarboxylation reactions, which take advantage of the high stability of CO₂, has been demonstrated by O'Hair and co-workers with the production of organometallics from carboxylates.⁴⁴⁻⁴⁷ One of the routes to the gas-phase syntheses of N≡U=O⁺ was endothermic CO₂ elimination from the isocyanate complex, UO₂(NCO)Cl₂⁻, to yield the chloride anion complex NUOCl₂⁻.⁴¹ The inverse of the computed potential energy profile for this transformation predicts that, in addition to being exothermic, insertion of CO₂ into NUOCl₂⁻ to yield UO₂(NCO)Cl₂⁻ should occur without any barriers above the reactant energies and should thus occur spontaneously under low-energy conditions. Such an insertion would result in activation of CO₂ with formation of a U-O bond and an NCO ligand bound to a uranyl cation core. This predicted activation of CO₂ was experimentally evaluated in the present work, with a goal of achieving the first insertion/activation of CO₂ into a gas-phase metal complex and furthermore providing an example of the principle of microscopic reversibility.^{48, 49}

Experimental

The general experimental approach has been described previously.⁵⁰ The anionic actinyl acetate complex, UO₂(NCO)Cl₂⁻, was produced by ESI of ethanol solutions containing 200 μM UO₂Cl₂ and 200 μM NaNCO. The nitrido actinyl complex, NUOCl₂⁻, was produced by collision induced dissociation of UO₂(NCO)Cl₂⁻ as previously described.⁴¹

The experiments were performed using an Agilent 6340 quadrupole ion trap mass spectrometer with MSⁿ collision-induced dissociation (CID) capability. The CID energy is an instrumental parameter that provides a qualitative indication of relative ion excitation. Ions in the trap can undergo ion-molecule reactions at ~300 K⁵¹ by applying a reaction time of up to 10 s. Anion mass spectra were acquired using the following parameters: solution flow rate, 60 μL/h; nebulizer gas pressure, 15 psi; capillary voltage offset and current, 4000 V and 19.5 nA; end plate voltage offset and current, -500 V and 100 nA; dry gas flow rate, 5 l/min; dry gas temperature, 325 °C; capillary exit, -300 V; skimmer, -15.0 V; octopole 1 and 2 DC, -13.3 and -9.6 V; octopole RF amplitude, 258; lens 1 and 2, 15 and 100 V; trap drive, 70. Nitrogen gas for

nebulization and drying was supplied from the boil-off of a liquid nitrogen Dewar. The background water pressure in the ion trap is estimated as $\sim 10^{-6}$ Torr;⁵² reproducibility of hydration rates of $\text{UO}_2(\text{OH})^+$ established that the water pressure was constant to within $<10\%$.⁵³ The helium buffer gas pressure in the trap is constant at $\sim 10^{-4}$ Torr. The ion trap has been modified to allow for the introduction of reagent gases through a leak valve. CO_2 gas (Airgas, 99.99%) was introduced into the ion trap to maintain a constant (unknown) pressure, estimated to be on the order of ca. 10^{-6} Torr on the basis of the increase in pressure measured by an ion gauge in the vacuum chamber outside of the ion trap.

Computational details

The potential energy profile (PEP) for the endothermic formation of CO_2 from the $\text{UO}_2(\text{NCO})\text{Cl}_2^-$ was previously reported.⁴¹ This PEP was computed within the frame of density functional theory, using the B3LYP hybrid functional,^{54,55} together with the Stuttgart-Dresden (so-called SDD) basis sets for uranium^{56,57} and the 6-311+G(2d) for the rest of the atoms^{58,59} (see reference 41 for further details). The PEP for the reverse reaction, i.e. the exothermic addition of CO_2 to NUOCl_2^- reported here was directly taken from the results reported in reference 41. In our previous publication, we focus exclusively on the potential energy profiles. With the aim to evaluate whether it is the energy or the free energy which determines reactivity under the experimental low-pressure bimolecular conditions, we here report additional information, i.e. the relative enthalpies and free energies at 298.15 K, which were taken directly from the Gaussian09 (revision C01)⁶⁰ thermochemistry outputs used to compute the PEP in reference 41.

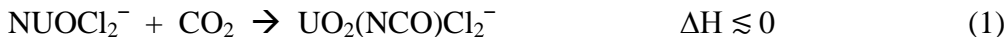
Results and Discussion

The computed PEP for exothermic addition of CO_2 to NUOCl_2^- is shown in Figure 1. The corresponding profiles obtained from relative enthalpies at 298.15 K differ from the PEPs shown in Figure 1 by $4 \text{ kJ}\cdot\text{mol}^{-1}$ or less, with the species generally further stabilized with respect to the $\text{NUOCl}_2^- + \text{CO}_2$ reactants (see Table 1). The very small value for TS3 is not included in Figure 1 because we were unable to localize it by optimization. The transformation between **Isomer 1** and the ground-state isomer is essentially barrierless, as was shown through a relaxed scan calculation (see page 328 and Figure S3 of ref.⁴¹).

As in previous experiments,⁴¹ the $\text{UO}_2(\text{NCO})\text{Cl}_2^-$ complex was isolated in the ion trap from all species originally formed by the ESI source in order to eliminate uranyl complexes with additional NCO ligands, as well as other uranyl and impurity species produced by ESI. As is seen in Figure S1, the yield of $\text{UO}_2(\text{NCO})\text{Cl}_2^-$ was lower than that of UO_2Cl_3^- . The assignment as $\text{UO}_2(\text{NCO})\text{Cl}_2^-$ was substantiated by the characteristic isotopic abundances of the three isotopomers, as well as by the characteristic chemistry. The key experimental results are shown in Figure 2. The top mass spectrum, Figure 2a, shows the formation of NUOCl_2^- by CID of $\text{UO}_2(\text{NCO})\text{Cl}_2^-$, as described previously.⁴¹ The most intense $\text{UO}_2(\text{NCO})^{35}\text{Cl}_2^-$ isotopomer at 382 m/z was isolated for CID, resulting in $\text{NUO}^{35}\text{Cl}_2^-$ at 338 m/z, and neutral CO_2 . The middle mass

spectrum, Figure 2b, is obtained after isolation of the $\text{NUO}^{35}\text{Cl}_2^-$ species. It shows the absence of any abundant reaction products, rather only a small peak at 356 m/z resulting from water addition after reaction of NUOCl_2^- with background gases in the ion trap for 0.05 s. The formulation of the water-addition peak as $\text{NUOCl}_2(\text{H}_2\text{O})^-$ does not imply knowledge that it is a hydrate rather than a hydrolysis product. Instead, we propose that this reaction product is likely the amide, $\text{UO}_2(\text{NH}_2)\text{Cl}_2^-$ (Figure S3). An additional minor peak in this spectrum is apparent at 357 m/z. As demonstrated in Figure S4, this product increases in intensity relative to that at 356 m/z at longer reaction times, suggesting that it derives from the presumed amide via hydrolysis to yield $\text{UO}_2(\text{OH})\text{Cl}_2^-$ and ammonia. The assumed reaction with two water molecules and the composition of this terminal product was confirmed by reaction of $\text{NU}^{16}\text{O}^{35}\text{Cl}_2^-$ with H_2^{18}O to yield $\text{U}^{16}\text{O}^{18}\text{O}_2\text{H}^{35}\text{Cl}_2^-$ at 361 m/z, the structure of which is presumably the uranyl hydroxide complex, $\text{UO}_2(\text{OH})\text{Cl}_2^-$ (see Figures S2-S4). Given that the reactions resulting in the minor peaks are ancillary to the primary results reported here, this intriguing chemistry was not further pursued in this work.

The key experimental result is shown in Figure 2c. After CO_2 has been added to the ion trap, the isolated NUOCl_2^- (338 m/z) is allowed to react for 0.05 s yielding an intense peak at 382 m/z, 44 m/z higher, demonstrating spontaneous addition of CO_2 . The minor peaks corresponding to water addition (356 m/z), and subsequent addition of another H atom (357 m/z), appear in this reaction spectrum at essentially the same yields as for reaction with background gases (water) in the ion trap for the same reaction time. The product branching ratio under these reaction conditions is 80% CO_2 addition and 20% H_2O addition. To confirm that the appearance of the 382 m/z peak results from a spontaneous exothermic reaction, the kinetics were measured by monitoring the decay of the reactant NUOCl_2^- as a function of time. The logarithmic decay plot is shown in Figure 3. The linearity of this plot indicates that the reaction is for thermalized NUOCl_2^- . The observed process is given by reaction (1).



In reaction (1), the composition of the product as a uranyl isocyanate dichloride anion complex is based on the predicted reversibility of the CID reaction.

The spontaneous addition of CO_2 to NUOCl_2^- is in accord with the PEPs in Figure 1. The lowest energy pathway (shown in blue) presents no barriers above the energy of the reactants, NUOCl_2^- and CO_2 . There is an alternative pathway (shown in red) that has a barrier, **TS2'**, computed to be only 1 $\text{kJ}\cdot\text{mol}^{-1}$ above the reactant asymptote. When considering relative enthalpies at 298.15 K, **TS2'** is found to be 4 $\text{kJ}\cdot\text{mol}^{-1}$ below the reactant asymptote. In view of the uncertainties associated with the PEP computed by DFT, and the possibility for slightly hyperthermal reactions in the ion trap, the spontaneous addition of CO_2 to NUOCl_2^- does not definitively confirm the lowest energy (blue) pathway, although the present results are most consistent with this pathway. The results do confirm the prediction that the addition reaction should proceed spontaneously at low ($< 10 \text{ kJ}\cdot\text{mol}^{-1}$) energy in the ion trap. For the association

product to remain intact the energy released by the reaction must be partially dissipated before dissociation back to the reactants can occur. The necessary cooling can be radiatively by photon emission and/or collisionally by interactions with low-energy atoms or molecules. In the present experiments, the helium in the ion trap at a pressure of ca. 10^{-4} Torr provides a means for collisional cooling of a sufficiently long-lived intermediate.

An attribute of gas-phase reactions between small ions and neutrals is the ability to accurately model the reaction mechanism, as with the PEP shown in Figure 1. For both of the viable pathways shown, the first step is formation of a weakly bound association complex, **Int.1**, which is only $16 \text{ kJ}\cdot\text{mol}^{-1}$ lower in energy than the reactant energies. This complex transforms over a small barrier at **TS1** to **Int.2**, which has both U-N and U-O bonding interactions and lies $70 \text{ kJ}\cdot\text{mol}^{-1}$ below the reactant energies. In the predicted lower-energy pathway, a C-O bond is cleaved and a C-N bond created to yield **Isomer 1** in which the produced isocyanate ligand is trans to one U=O bond and cis to another U=O bond. Rearrangement to the uranyl isocyanate proceeds via a very low energy barrier, **TS3**. In the computed higher-energy pathway, which cannot be excluded on the basis of the experimental results but is less consistent with the observed spontaneous reaction, **Int.2** directly rearranges to the uranyl isocyanate product via **TS2'**, which lies very close in energy to the reactant energies. The low barriers for addition of CO_2 to NUOCl_2^- can be attributed to the retention of strong U-O and U-N bonds in all of the transition states. The substantial exothermicity of the net reaction, $-256 \text{ kJ}\cdot\text{mol}^{-1}$, despite the disrupted bonding in CO_2 , is similarly attributed to the presence of strong U-O and U-N bonds in the isocyanate product.

The present results demonstrate that the computed pathway for endothermic decarboxylation, as previously reported,⁴¹ is the same as that for exothermic CO_2 activation. This is an example of the principle of microscopic reversibility that was explicitly postulated by Tolman in 1925.⁴⁸ The following conclusion from Marcelin, who had previously invoked this unnamed principle in his theory of chemical kinetics,⁶¹ is from Tolman:⁴⁸ “the energy of the molecules in the activated states which lead to reaction has to be the same for two opposing reactions”. This concept is clearly revealed by the present results.

There are several cases of CO_2 activation by uranium complexes, including by uranium nitrides.¹⁴⁻²⁴ Most of this chemistry involves reductive insertion of CO_2 into U(III) or U(IV) complexes without cleavage of a C-O bond and is thus not activation per se. To the best of our knowledge, this is the first report of activation of CO_2 by a U(VI) complex and of activation of a $\text{U}\equiv\text{N}$ bond by CO_2 to yield uranyl.

It is generally accepted that the reaction energy, ΔE , is the pertinent thermodynamic parameter in determining whether or not a low-pressure bimolecular reaction proceeds. There has however been discussion as to the potential role of entropy, with the implication that the free energy, ΔG , can be a pertinent parameter under some conditions.^{62, 63} Figure 4 shows the computed free energy profiles (FEPs) for the two alternative reaction pathways, here plotted as relative free energies at 298 K (B3LYP/SDD:6-311+G(2d)).⁴¹ Although the net reaction is substantially exoergic, it is apparent that there are significant ($>20 \text{ kJ}\cdot\text{mol}^{-1}$) barriers above the

free energy of the reactants, such that the reaction should not proceed spontaneously if ΔG is the pertinent energy. The substantial disparity between the energy and free energy profiles for this reaction is a result of transforming two gas-phase particles to one, which results in a substantially unfavorable entropy for the process. The computed ΔS_{298} for reaction (1) is $-124 \text{ J.K}^{-1}.\text{mol}^{-1}$, a value that is consistent with the loss of three translational and two rotational degrees of freedom upon converting two gas-phase molecules to one. The unfavorable entropy effect is manifested throughout the FEPs (Figure 4), which are uniformly higher in energy (by 35-47 kJ.mol^{-1}) than the corresponding PEPs (Figure 1), except for the separated reactants for which both energies are by definition zero. The results demonstrate that the reaction energy (PEP), rather than free energy (FEP), is the relevant parameter under conditions of low-pressure bimolecular reactions.

Conclusions

It was previously demonstrated that the gas-phase uranyl anion complex $\text{UO}_2(\text{NCO})\text{Cl}_2^-$ endothermically eliminates CO_2 to furnish NUOCl_2^- in which a $\text{U}=\text{O}$ bond has been activated to produce a terminal $\text{U}\equiv\text{N}$ bond. The computed PEP for this endothermic fragmentation predicted that there should be no energy barriers above the reactant energies for the reverse exothermic addition of CO_2 to NUOCl_2^- . This prediction has now been validated by the observation in the present work of the spontaneous addition of CO_2 to NUOCl_2^- to yield the decarboxylation precursor $\text{UO}_2(\text{NCO})\text{Cl}_2^-$. The present results provide a demonstration of microscopic reversibility. Although the results are consistent with both computed PEPs, they are in better accord with the pathway with lower energy barriers, which proceeds via an unusual isomer of $\text{UO}_2(\text{NCO})\text{Cl}_2^-$ in which there is an isocyanate ligand trans to one $\text{U}=\text{O}$ bond and cis to the second $\text{U}=\text{O}$ bond. This isomer is surprisingly only 114 kJ.mol^{-1} higher in energy than the ground state structure of a uranyl moiety with three equatorial (cis) anion ligands. The FEP predicts that the observed reaction should not occur spontaneously under thermal conditions, providing a demonstration that it is ΔE rather than ΔG that is the pertinent thermodynamic parameter under bimolecular reaction conditions such as in the present experiments.

Although it is certainly possible to adsorb CO_2 onto cold gas-phase complexes, the type of addition process observed here is rare, if not unprecedented, reflecting the inert nature of carbon dioxide. There have been several reports of insertion of CO_2 into U-N (and other uranium-main group element) bonds in condensed phase complexes; however, these so-called “activation” processes generally involve oxidative insertion without cleavage of a C-O bond. The true activation of CO_2 , i.e. C-O bond cleavage, observed in the present work is enabled by the creation of a strong $\text{U}=\text{O}$ bond and an isocyanate ligand that results in a U-NCO linkage. The relatively low kinetic barriers that enable the process to occur spontaneously reflect that the two U-O bonds and one U-N bond are retained throughout. This unprecedented gas-phase chemistry enables molecular-scale mechanistic insights that could motivate new condensed-phase synthetic routes toward CO_2 activation by uranium nitride complexes.

Supporting Information

ESI mass spectrum showing $\text{UO}_2(\text{NCO})\text{Cl}_2^-$. Mass spectra for reactions of NUOCl_2^- with H_2^{16}O and H_2^{18}O . Possible products from the sequential reaction of NUOCl_2^- with two water molecules. Mass spectra used to obtain kinetics plot in Figure 3.

Acknowledgements

This work was supported by the U.S. Department of Energy, Office of Basic Energy Sciences, Heavy Element Chemistry Program, at LBNL under Contract No. DE-AC02-05CH11231 (P.D.D. and J.K.G.) and at the University of Utah by grant no. DE-SC0012249 (P.B.A.), and by Università della Calabria, Italy (M.C.M.). This research used resources of the National Energy Research Scientific Computing Center, which is supported by the Office of Science of the U.S. D.O.E. under Contract No. DE-AC02-05CH11231.

References

1. S. G. Lias, J. E. Bartmess, J. F. Liebman, J. L. Holmes, R. D. Levin and W. G. Mallard, *J Phys Chem Ref Data*, 1988, **17**, 1-861.
2. R. Barker, *J Appl Chem Biotechn*, 1973, **23**, 733-742.
3. X. L. Yin and J. R. Moss, *Coordin Chem Rev*, 1999, **181**, 27-59.
4. W. J. Evans, D. B. Rego, J. W. Ziller, A. G. DiPasquale and A. L. Rheingold, *Organometallics*, 2007, **26**, 4737-4745.
5. W. Sattler and G. Parkin, *J Am Chem Soc*, 2012, **134**, 17462-17465.
6. M. Vogt, M. Gargir, M. A. Iron, Y. Diskin-Posner, Y. Ben-David and D. Milstein, *Chem-Eur J*, 2012, **18**, 9194-9197.
7. M. Torrent-Sucarrat and A. J. C. Varandas, *J Phys Chem A*, 2014, **118**, 12256-12261.
8. K. Huang, C. L. Sun and Z. J. Shi, *Chem Soc Rev*, 2011, **40**, 2435-2452.
9. Z. Z. Yang, L. N. He, J. Gao, A. H. Liu and B. Yu, *Energ Environ Sci*, 2012, **5**, 6602-6639.
10. A. Pinaka and G. C. Vougioukalakis, *Coordin Chem Rev*, 2015, **288**, 69-97.
11. J. S. Silvia and C. C. Cummins, *J Am Chem Soc*, 2010, **132**, 2169-2171.
12. A. J. Keane, W. S. Farrell, B. L. Yonke, P. Y. Zavalij and L. R. Sita, *Angew Chem Int Edit*, 2015, **54**, 10220-10224.
13. T. Andrea and M. S. Eisen, *Chem Soc Rev*, 2008, **37**, 550-567.
14. O. P. Lam and K. Meyer, *Polyhedron*, 2012, **32**, 1-9.
15. B. M. Gardner and S. T. Liddle, *Eur J Inorg Chem*, 2013, **2013**, 3753-3770.
16. H. S. La Pierre and K. Meyer, *Prog Inorg Chem*, 2014, **58**, 303-415.
17. K. W. Bagnall and E. Yanir, *J Inorg Nucl Chem*, 1974, **36**, 777-779.
18. I. Castro-Rodriguez, H. Nakai, L. N. Zakharov, A. L. Rheingold and K. Meyer, *Science*, 2004, **305**, 1757-1759.
19. S. C. Bart, C. Anthon, F. W. Heinemann, E. Bill, N. M. Edelstein and K. Meyer, *J Am Chem Soc*, 2008, **130**, 12536-12546.
20. S. M. Mansell, N. Kaltsoyannis and P. L. Arnold, *J Am Chem Soc*, 2011, **133**, 9036-9051.
21. P. L. Arnold, Z. R. Turner, A. I. Germeroth, I. J. Casely, G. S. Nichol, R. Bellabarba and R. P. Tooze, *Dalton Trans*, 2013, **42**, 1333-1337.
22. E. M. Matson, P. E. Fanwick and S. C. Bart, *Organometallics*, 2011, **30**, 5753-5762.
23. R. J. Kahan, F. G. N. Cloke, S. M. Roe and F. Nief, *New J Chem*, 2015, **39**, 7602-7607.

24. C. L. Webster, J. W. Ziller and W. J. Evans, *Organometallics*, 2014, **33**, 433-436.
25. M. M. Kappes and R. H. Staley, *J Phys Chem*, 1981, **85**, 942-944.
26. D. E. Lessen, R. L. Asher and P. J. Brucat, *J Chem Phys*, 1991, **95**, 1414-1416.
27. G. K. Koyanagi and D. K. Bohme, *J Phys Chem A*, 2006, **110**, 1232-1241.
28. M. R. Sievers and P. B. Armentrout, *J Chem Phys*, 1995, **102**, 754-762.
29. M. R. Sievers and P. B. Armentrout, *Int J Mass Spectrom*, 1998, **180**, 103-115.
30. M. R. Sievers and P. B. Armentrout, *Inorg Chem*, 1999, **38**, 397-402.
31. P. B. Armentrout and J. L. Beauchamp, *Chemical Physics*, 1980, **50**, 27-36.
32. M. Santos, J. Marçalo, A. P. de Matos, J. K. Gibson and R. G. Haire, *J Phys Chem A*, 2002, **106**, 7190-7194.
33. J. B. Griffin and P. B. Armentrout, *Journal of Chemical Physics*, 1997, **107**, 5345-5355.
34. J. B. Griffin and P. B. Armentrout, *Journal of Chemical Physics*, 1998, **108**, 8075-8083.
35. J. Schwarz and H. Schwarz, *Organometallics*, 1994, **13**, 1518-1520.
36. R. Wesendrup and H. Schwarz, *Angewandte Chemie-International Edition in English*, 1995, **34**, 2033-2035.
37. D. Schröder, H. Schwarz, S. Schenk and E. Anders, *Angew Chem Int Edit*, 2003, **42**, 5087-5090.
38. J. L. Li, P. Gonzalez-Navarrete, M. Schlangen and H. Schwarz, *Chem-Eur J*, 2015, **21**, 7780-7789.
39. S. Y. Tang, N. J. Rijs, J. L. Li, M. Schlangen and H. Schwarz, *Chem-Eur J*, 2015, **21**, 8483-8490.
40. J. Marçalo and J. K. Gibson, *J Phys Chem A*, 2009, **113**, 12599-12606.
41. Y. Gong, V. Vallet, M. C. Michelini, D. Rios and J. K. Gibson, *J Phys Chem A*, 2014, **118**, 325-330.
42. M. J. Van Stipdonk, M. C. Michelini, A. Plaviak, D. Martin and J. K. Gibson, *J Phys Chem A*, 2014, **118**, 7838-7846.
43. T. W. Hayton, *Chem Commun*, 2013, **49**, 2956-2973.
44. R. A. J. O'Hair, A. K. Vrkic and P. F. James, *J Am Chem Soc*, 2004, **126**, 12173-12183.
45. N. J. Rijs and R. A. J. O'Hair, *Organometallics*, 2009, **28**, 2684-2692.
46. L. O. Sraj, G. N. Khairallah, G. da Silva and R. A. J. O'Hair, *Organometallics*, 2012, **31**, 1801-1807.
47. R. A. J. O'Hair and N. J. Rijs, *Accounts Chem Res*, 2015, **48**, 329-340.
48. R. C. Tolman, *Proceedings of the National Academy of Sciences of the United States of America*, 1925, **11**, 436-439.
49. R. L. Burwell and R. G. Pearson, *Journal of Physical Chemistry*, 1966, **70**, 300-302.
50. D. Rios, P. X. Rutkowski, D. K. Shuh, T. H. Bray, J. K. Gibson and M. J. Van Stipdonk, *J Mass Spectrom*, 2011, **46**, 1247-1254.
51. S. Gronert, *J Am Soc Mass Spectr*, 1998, **9**, 845-848.
52. P. X. Rutkowski, M. C. Michelini, T. H. Bray, N. Russo, J. Marçalo and J. K. Gibson, *Theor Chem Acc*, 2011, **129**, 575-592.
53. D. Rios, M. C. Michelini, A. F. Lucena, J. Marçalo, T. H. Bray and J. K. Gibson, *Inorg Chem*, 2012, **51**, 6603-6614.
54. C. T. Lee, W. T. Yang and R. G. Parr, *Phys Rev B*, 1988, **37**, 785-789.
55. A. D. Becke, *J Chem Phys*, 1993, **98**, 5648-5652.
56. W. Kuchle, M. Dolg, H. Stoll and H. Preuss, *J Chem Phys*, 1994, **100**, 7535-7542.
57. X. Y. Cao, M. Dolg and H. Stoll, *J Chem Phys*, 2003, **118**, 487-496.
58. R. Krishnan, J. S. Binkley, R. Seeger and J. A. Pople, *J Chem Phys*, 1980, **72**, 650-654.
59. T. Clark, J. Chandrasekhar, G. W. Spitznagel and P. V. Schleyer, *J Comput Chem*, 1983, **4**, 294-301.
60. Gaussian 09, Revision C.01 G. W. T. M. J. Frisch, H. B. Schlegel, G. E. Scuseria, M. A. Robb, J. R. Cheeseman, G. Scalmani, V. Barone, B. Mennucci, G. A. Petersson, H. Nakatsuji, M. Caricato, X. Li, H. P. Hratchian, A. F. Izmaylov, J. Bloino, G. Zheng, J. L. Sonnenberg, M. Hada, M. Ehara, K. Toyota, R. Fukuda, J. Hasegawa, M. Ishida, T. Nakajima, Y. Honda, O. Kitao, H. Nakai, T. Vreven, J. A. Montgomery, Jr., J. E. Peralta, F. Ogliaro, M. Bearpark, J. J. Heyd, E. Brothers, K. N. Kudin, V. N.

- Staroverov, R. Kobayashi, J. Normand, K. Raghavachari, A. Rendell, J. C. Burant, S. S. Iyengar, J. Tomasi, M. Cossi, N. Rega, J. M. Millam, M. Klene, J. E. Knox, J. B. Cross, V. Bakken, C. Adamo, J. Jaramillo, R. Gomperts, R. E. Stratmann, O. Yazyev, A. J. Austin, R. Cammi, C. Pomelli, J. W. Ochterski, R. L. Martin, K. Morokuma, V. G. Zakrzewski, G. A. Voth, P. Salvador, J. J. Dannenberg, S. Dapprich, A. D. Daniels, Ö. Farkas, J. B. Foresman, J. V. Ortiz, J. Cioslowski, and D. J. Fox, Gaussian Inc., Wallingford CT, 2009.
61. R. Marceline, *Annales de Physique*, 1915, **3**, 120-231.
62. K. K. Irikura, *J Am Chem Soc*, 1999, **121**, 7689-7695.
63. G. Innorta, S. Torroni, A. Maranzana and G. Tonachini, *J Organomet Chem*, 2001, **626**, 24-31.

Table 1. Calculated energies of the species involved in reaction 1.^a

	ΔE_0	ΔH_{298}	ΔG_{298}
Int. 1	-16	-18	24
TS1	-15	-17	23
Int. 2	-70	-73	-26
TS2	-24	-27	21
TS2'	1	-4	48
Isomer 1	-142	-141	-107
UO₂(NCO)Cl₂⁻	-256	-256	-219

^a In kJ.mol⁻¹. ΔE_0 are the relative energies at 0 K (including the zero point energy correction), ΔH_{298} are the relative enthalpies at 298.15 K, and ΔG_{298} are the relative free energies at 298.15 K. The energy of TS3 was not determined, as discussed in ref.⁴¹

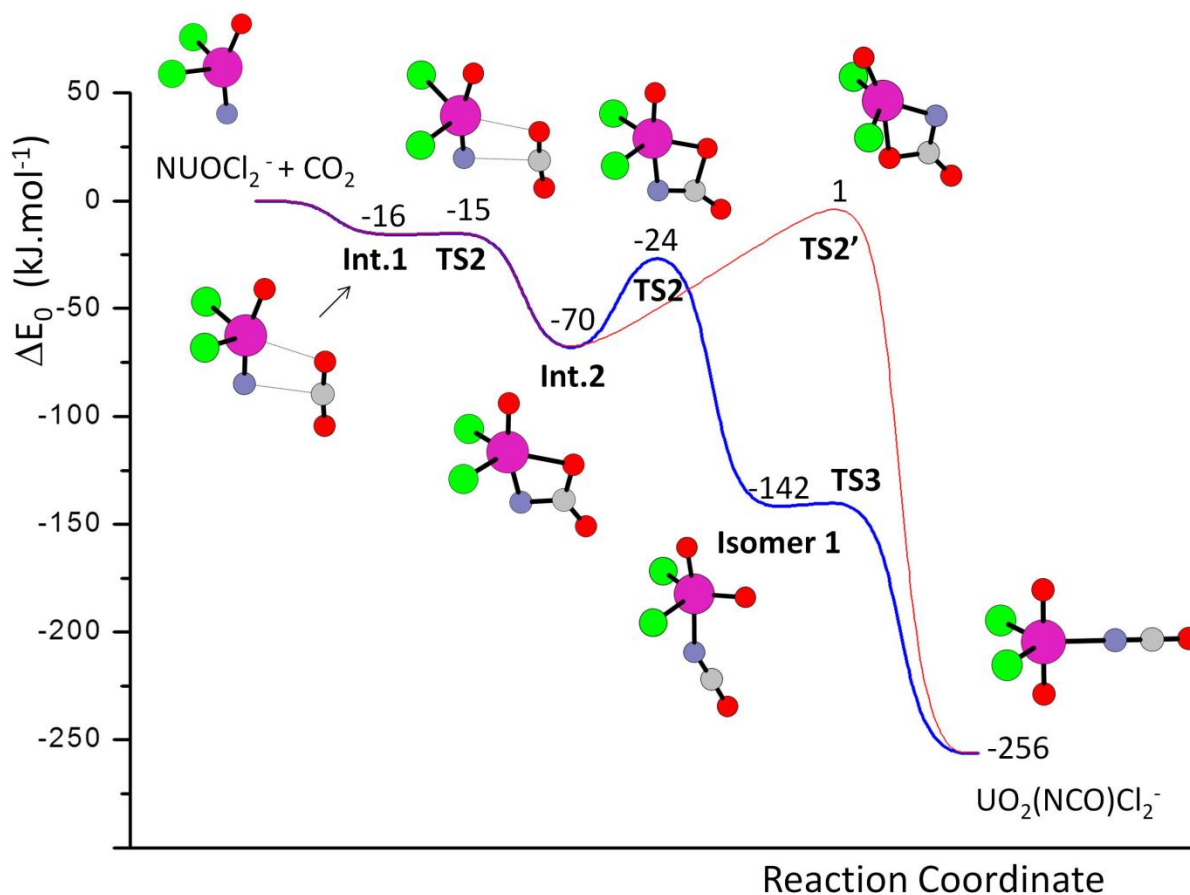


Figure 1. Computed PEP for exothermic addition of CO_2 to NUOCl_2^- , reaction 1. Energies in $\text{kJ}\cdot\text{mol}^{-1}$ relative to reactants are shown. This PEP is simply the reverse of that previously reported for endothermic elimination of CO_2 from $\text{UO}_2(\text{NCO})\text{Cl}_2^-$.⁴¹ Purple – uranium, green – chlorine, red – oxygen, blue – nitrogen, grey – carbon. For details regarding TS3, which presents a very small barrier, see page 328 and Figure S3 of reference⁴¹.

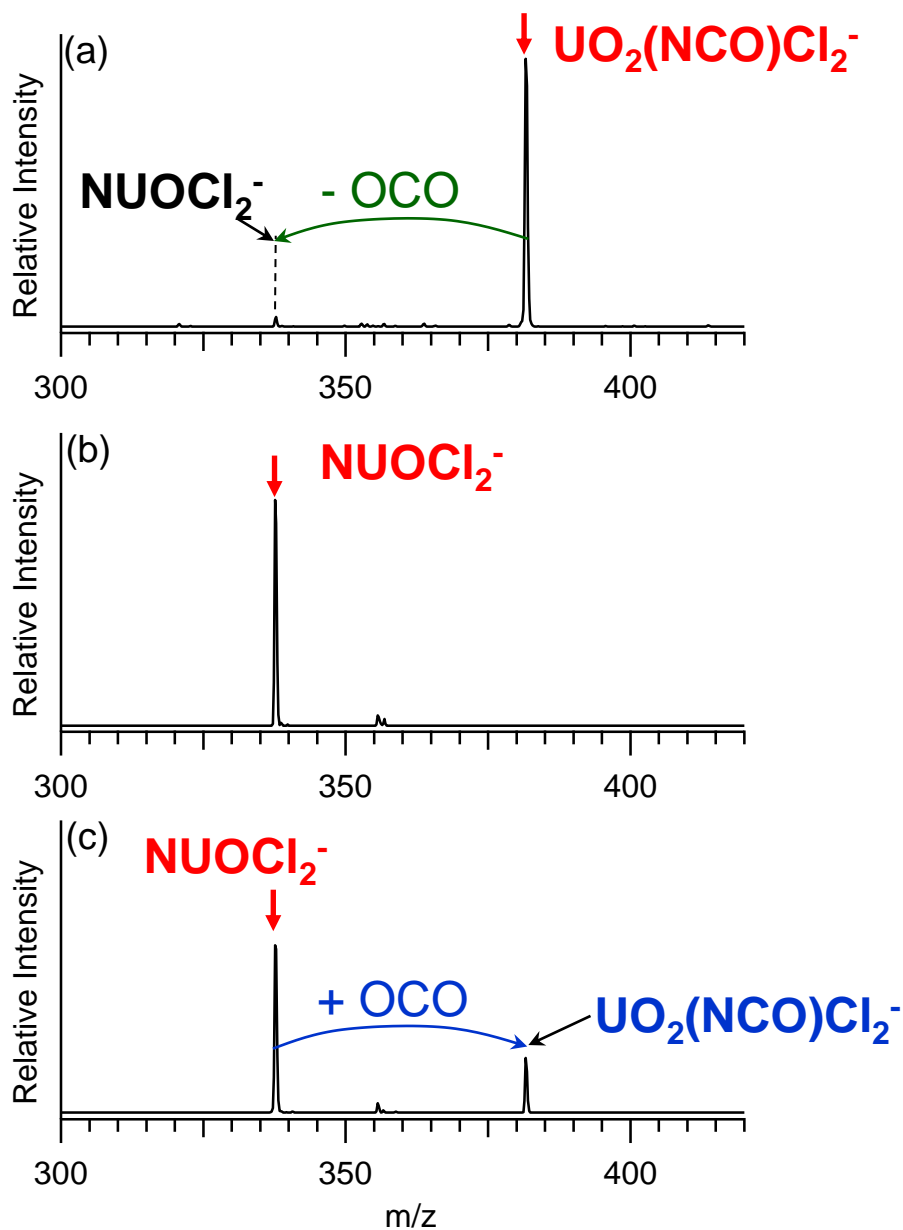


Figure 2. Mass spectra for (a) formation of NUOCl_2^- by CID of $\text{UO}_2(\text{NCO})\text{Cl}_2^-$; (b) reaction of isolated NUOCl_2^- with background gases in the ion trap for 0.05 seconds; (c) reaction with background gases and added CO_2 in the ion trap for 0.05 seconds. The minor peak at 356 m/z in (b) and (c) presumably results from addition of water to produce $\text{UO}_2(\text{NH}_2)\text{Cl}_2^-$. The minor peak at 357 m/z in (b) is attributed to subsequent hydrolysis to yield $\text{UO}_2(\text{OH})\text{Cl}_2^-$ and ammonia.

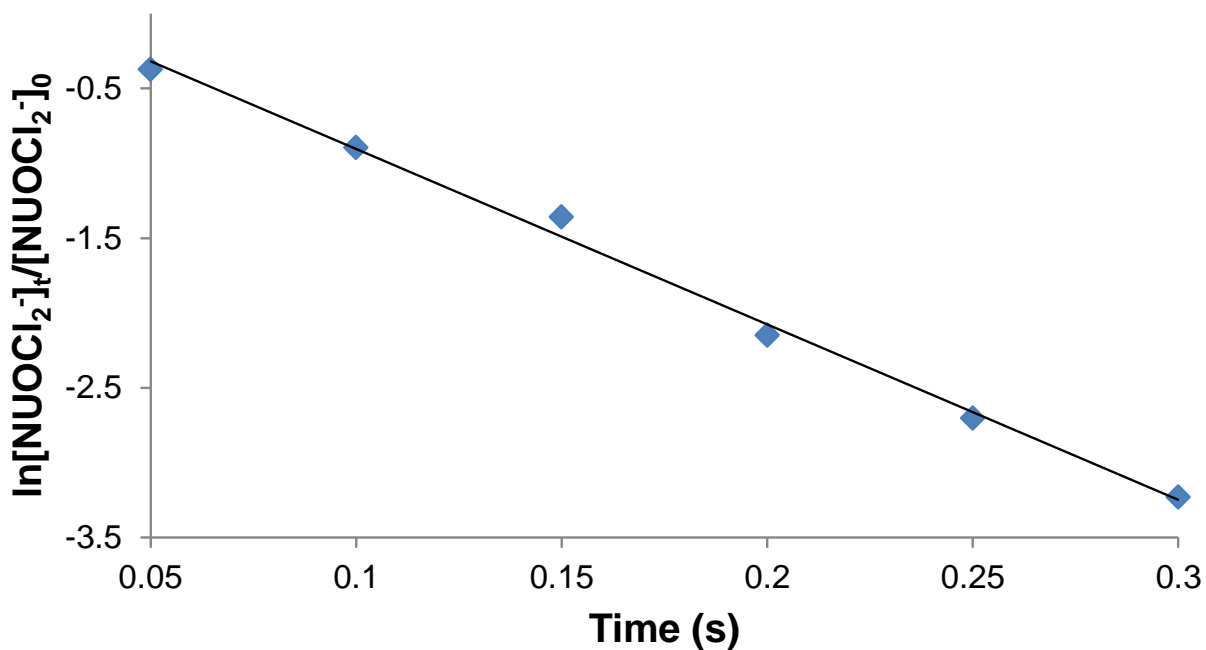


Figure 3. Logarithmic decay kinetics plot for pseudo-first order reaction of NUOCl_2^- with CO_2 and background water. The measured composite pseudo-first order reaction rate is 11.7 s^{-1} ($R^2 = 0.996$). The mass spectra used to obtain this plot are shown in Figure S2. The product branching ratios are 80% CO_2 addition and 20% H_2O addition.

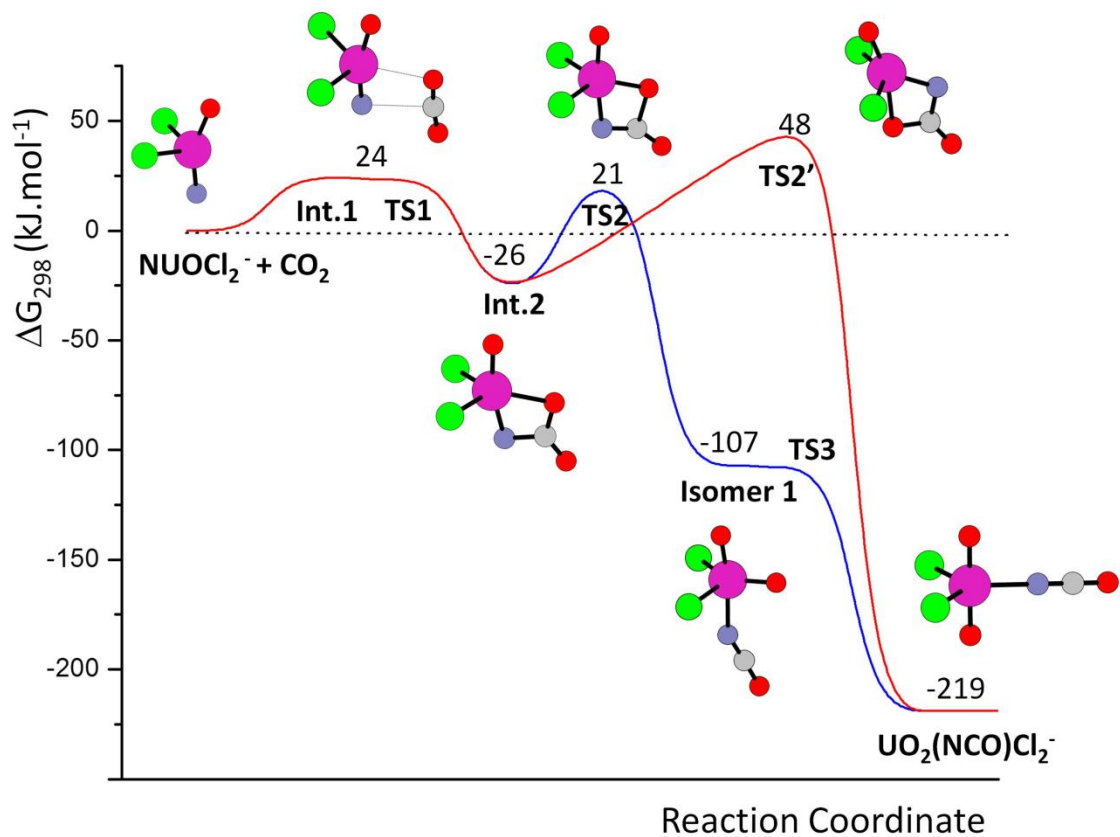


Figure 4. Computed free energy profile (FEP) for exoergic addition of CO₂ to NUOCl₂⁻. This energy profile is the same as that shown in Figure 1 except that the energy scale is ΔG_{298} rather than ΔE_0 . Purple – uranium, green – chlorine, red – oxygen, blue – nitrogen, grey – carbon.